

# Alternative splicing of CTP:phosphoethanolamine cytidyltransferase produces two isoforms that differ in catalytic properties

Angela Tie and Marica Bakovic<sup>1</sup>

Department of Human Health and Nutritional Sciences, University of Guelph, Guelph, Ontario N1G 2W1, Canada

**Abstract** CTP:phosphoethanolamine cytidyltransferase (Pcyt2) catalyzes the rate-controlling reaction of the CDP-ethanolamine (Kennedy) pathway. We have previously established that Pcyt2 is encoded by a single gene that can be alternatively spliced from an internal exon into two transcripts, designated Pcyt2 $\alpha$  and Pcyt2 $\beta$ . Little is currently known about the regulation of Pcyt2. Here, we functionally express both murine Pcyt2 (mPcyt2) transcripts and investigate the roles of the two proteins in the regulation of mPcyt2 activity. We demonstrate that the tagged and purified  $\alpha$  and  $\beta$  proteins differ significantly in their kinetic properties. The  $K_m$  of mPcyt2 $\alpha$  for phosphoethanolamine was 318.4  $\mu$ M, compared with 140.3  $\mu$ M for mPcyt2 $\beta$ . The maximal velocities of the  $\alpha$  and  $\beta$  isoforms at saturating conditions for both substrates were 138.0 and 114.4 nmol/min/ $\mu$ mol enzyme, respectively. When phosphoethanolamine was used at a fixed concentration of 1 mM, the  $K_m$  of mPcyt2 $\alpha$  for CTP was 102.0  $\mu$ M and that of mPcyt2 $\beta$  was 84.09  $\mu$ M. Using a combination of nondenaturing PAGE, gel filtration chromatography, and immunoprecipitation, we provide evidence that mPcyt2 $\alpha$  and mPcyt2 $\beta$  proteins can form both homodimeric and heterodimeric complexes. We show that alternative splicing of the mPcyt2 transcript is ubiquitous but could also be regulated in a tissue-specific manner, producing a variable ratio of mPcyt2 $\alpha$ /mPcyt2 $\beta$  mRNAs. The expression of two distinct protein isoforms maybe an important mechanism by which Pcyt2 activity is regulated.—Tie, A., and M. Bakovic. Alternative splicing of CTP:phosphoethanolamine cytidyltransferase produces two isoforms that differ in catalytic properties. *J. Lipid Res.* 2007. 48: 2172–2181.

**Supplementary key words** cytidyltransferase • CDP-ethanolamine • phospholipids • dimerization

CTP:phosphoethanolamine cytidyltransferase (Pcyt2) catalyzes the formation of CDP-ethanolamine from phosphoethanolamine and CTP in the rate-controlling reac-

tion of the CDP-ethanolamine (Kennedy) pathway (1–3). This pathway is known as the sole route of de novo phosphatidylethanolamine (PE) synthesis in mammalian cells. PE is also produced by the mitochondrial decarboxylation of phosphatidylserine (4) and by base exchange with phosphatidylserine or phosphatidylcholine (5). PE is an important structural phospholipid in mammalian cell membranes, in part because of its tendency to form non-lamellar structures (6). These unique biophysical properties of PE confer a specialized role in membrane fusion-mediated events, including cytokinesis (7), endocytosis (8), and vesiculation (9). In autophagy, covalent linkage of PE to the C-terminal arginine of Apg8 is necessary for the association of this ubiquitin-like protein with the autophagosomal membrane (10). PE is a known reservoir of the potent biological mediator, arachidonic acid. The phospholipase A<sub>2</sub>, cPLA<sub>2</sub> $\gamma$ , is a microsomal enzyme that shows preferential activity toward arachidonic acid at the *sn*-2 position of PE (11). This selective arachidonic acid release is seen in response to agents of oxidative stress, such as H<sub>2</sub>O<sub>2</sub> (11).

Specialized ether derivatives of PE known as plasmalogens constitute up to 18% of total phospholipid mass (12), with the highest content being found in brain myelin (13). The physiological functions of plasmalogens have not been well characterized, and their study is complicated by the multitude of metabolic abnormalities that accompany plasmalogen deficiency in severe inherited peroxisomal disorders such as Zellweger's syndrome (14). The importance of the CDP-ethanolamine pathway was highlighted by the observation that ethanolamine was used in the synthesis of both PE and plasmalogens, but no plasmalogens could be derived from products of phosphatidylserine decarboxylation (12).

Although CTP:phosphocholine cytidyltransferase (Pcyt1), the analogous enzyme of the CDP-choline

Manuscript received 19 December 2006 and in revised form 9 May 2007 and in re-revised form 6 July 2007.

Published, JLR Papers in Press, July 23, 2007.  
DOI 10.1194/jlr.M600536-JLR200

Abbreviations: Ni-NTA, nickel-nitrilotriacetic acid agarose; Pcyt2, CTP:phosphoethanolamine cytidyltransferase; PE, phosphatidylethanolamine.

<sup>1</sup>To whom correspondence should be addressed.

e-mail: mbakovic@uoguelph.ca

Copyright © 2007 by the American Society for Biochemistry and Molecular Biology, Inc.

pathway, has been studied extensively (15, 16), considerably less is known about Pcyt2. Unlike Pcyt1, the Pcyt2 protein lacks sufficient hydrophobic domains to span a membrane (17), and lipid association is not required for the activation of Pcyt2 (18). Pcyt2 protein has been purified from rat liver (5, 18, 19), and several of its properties indicate a dimeric structure, with two phosphoethanolamine binding sites within each monomer unit (5, 19). The yeast gene (17) and human (20) and rat (21) cDNAs have been cloned and characterized. We reported on the genomic organization and differential splicing of murine Pcyt2 (mPcyt2), designating two mRNA transcripts ( $\alpha$  and  $\beta$ ). The resulting proteins differ by an 18 amino acid peptide sequence encoded by exon 7 of the Pcyt2 gene and present only in the  $\alpha$  form. We found that an identical "exon-skipping" mechanism is conserved in a wide range of species, suggesting that both transcripts have physiological relevance (22). Nevertheless, information regarding the expression, interaction, and function of the two distinct proteins is lacking. Here, we report the expression and purification of epitope-tagged mPcyt2 $\alpha$  and mPcyt2 $\beta$  proteins that differ in catalytic activity and kinetic parameters. We show variations in the tissue expression pattern of the two isoforms and present the first evidence that mPcyt2 $\alpha$  and mPcyt2 $\beta$  are both functional proteins that can form products of homodimeric and heterodimeric association.

## MATERIALS AND METHODS

### Construction and expression of epitope-tagged mPcyt2 $\alpha$ and mPcyt2 $\beta$ cDNAs

Plasmids containing the mPcyt2 $\alpha$  and mPcyt2 $\beta$  cDNAs (GenBank accession numbers BC003473 and BU557590) were purchased from the American Type Culture Collection. The inserts corresponding to each cDNA coding region were subcloned into the pcDNA4/myc-His vector (Invitrogen), which adds the myc epitope and polyhistidine tags to the C terminus of the expressed protein. In brief, the cDNA coding regions of mPcyt2 $\alpha$  and mPcyt2 $\beta$  were amplified using PCR primers designed to add the *EcoRV* and *XhoI* restriction sites to the 5' and 3' ends of the cDNAs, respectively. The translation termination codons were deleted so that the myc and Hisx6 tags would be added onto the mPcyt2 proteins. Amplified cDNAs were subcloned into the pGEM-T Easy vector (Promega), then removed by restriction digestion with *EcoRV* and *XhoI* and subcloned into the pcDNA4/myc-His vector. These two constructs are referred to as mPcyt2 $\alpha$ -myc-His and mPcyt2 $\beta$ -myc-His. The mPcyt2 $\alpha$  cDNA was also cloned into the pcDNA3.1/V5-His vector (Invitrogen), which adds the C-terminal V5 epitope and polyhistidine tags. The cDNA inserts in all final constructs were sequenced at the Guelph Molecular Supercenter to ensure that coding errors had not occurred. COS-7 cells were grown in DMEM with 10% fetal bovine serum. For enzyme activity and Western blotting, cells in 60 mm dishes were transfected with 5  $\mu$ g of empty vector, mPcyt2 $\alpha$ -myc-His, or mPcyt2 $\beta$ -myc-His constructs using 20  $\mu$ l of Lipofectamine (Invitrogen). Forty-eight hours after transfection, the cells were harvested in lysis buffer [25 mM Tris-phosphate, pH 7.8, 15% glycerol, 1% Triton X-100, 8 mM MgCl<sub>2</sub>, 1 mM dithiothreitol, 10  $\mu$ g/ml each leupeptin, aprotinin, and soybean trypsin inhibitor, 0.5 mM PMSF, 1  $\mu$ g/ml pepstatin A, 0.01% Nonidet P-40, and 0.2% phosphatase inhibitor cocktail II (Sigma)].

### Enzyme activity assays

Total cell lysates were prepared by harvesting cells in lysis buffer as described above. After centrifugation at 13,000 *g* and 4°C to pellet cell debris, the supernatants were assayed for mPcyt2 activity as described (23), except that commercially available [<sup>14</sup>C]phosphoethanolamine (American Radiolabeled Chemicals) was used at a final specific activity of 2  $\mu$ Ci/ $\mu$ mol. The final concentrations of phosphoethanolamine and CTP were 1 and 2 mM, respectively. All reactions were incubated at 37°C for 15 min followed by boiling for 2 min to inactivate the enzyme. CDP-ethanolamine and phosphoethanolamine standards were added to the samples and resolved on Silica Gel G plates in a solvent system of methanol/0.5% NaCl/ammonia (50:50:5). Individual spots were visualized using 2% ninhydrin in 95% ethanol, then scraped and subjected to liquid scintillation analysis. Three measurements were taken from each of three independent transfections.

### Radiolabeling with [<sup>14</sup>C]ethanolamine

COS-7 cells were grown on six-well plates and transfected with 2.5  $\mu$ g of plasmid DNA (empty vector, mPcyt2 $\alpha$ -myc-His, or mPcyt2 $\beta$ -myc-His) using 10  $\mu$ l of Lipofectamine. Forty-six hours after transfection, the cells were preconditioned for 2 h in DMEM containing 50  $\mu$ M ethanolamine, followed by 30 min of labeling with [<sup>14</sup>C]ethanolamine (0.2  $\mu$ Ci/well) in the presence of 50  $\mu$ M unlabeled ethanolamine. Cells were then washed twice in ice-cold PBS-A and harvested by trypsinization. The lipid and water-soluble fractions were separated by the method of Bligh and Dyer (24), and the radiolabeled ethanolamine, phosphoethanolamine, and CDP-ethanolamine in the methanol-water phase were separated and analyzed as described above. Three experiments were performed in triplicate. Total ethanolamine incorporation into PE was determined by evaporation of the entire chloroform phase under nitrogen, followed by the separation of PE from lyso-PE in a TLC system of chloroform-methanol-ammonia (65:35:5). Spots corresponding to PE and lyso-PE standards were scraped and subjected to liquid scintillation analysis. Because the contribution of lyso-PE was negligible, only PE was considered in the analysis. PE analysis was performed twice in duplicate.

### Purification of expressed mPcyt2 $\alpha$ and mPcyt2 $\beta$ proteins

COS-7 cells in 100 mm dishes were transfected with 16  $\mu$ g of either mPcyt2 $\alpha$ -myc-His or mPcyt2 $\beta$ -myc-His using 20  $\mu$ l of Lipofectamine (Invitrogen). After 48 h, cells were harvested by trypsinization and resuspended in lysis buffer (50 mM NaH<sub>2</sub>PO<sub>4</sub>, 300 mM NaCl, 10 mM imidazole, and 1% Triton X-100, pH 8.0) with protease and phosphatase inhibitor cocktails (Sigma). Cells were lysed by rocking at 4°C for 10 min and centrifuged at 4°C and 13,000 *g* for 10 min. For every 1 ml of lysis buffer used, 50  $\mu$ l of Ni-NTA Superflow nickel-charged resin (Qiagen) was added to the supernatant (cleared lysate) and allowed to bind with rocking at 4°C for 90 min. The sample mixture was loaded onto a chromatography column, and the unbound fraction was allowed to flow through by gravity. The resin was washed four times with 50 mM NaH<sub>2</sub>PO<sub>4</sub>, 300 mM NaCl, and 20 mM imidazole (pH 8.0). Bound protein was eluted multiple times with 100  $\mu$ l of elution buffer (50 mM NaH<sub>2</sub>PO<sub>4</sub>, 300 mM NaCl, and 250 mM imidazole, pH 8.0). The cleared lysate, unbound fraction, washes, and eluted fractions were analyzed by SDS-PAGE and Coomassie Brilliant Blue staining. Eluted fractions containing histidine-tagged protein were pooled and dialyzed overnight against 500 volumes of 20 mM Tris-HCl, 0.5 mM EDTA, 2 mM dithioerythritol, and 5% (v/v) ethylene glycol. SDS-PAGE and Coomassie Brilliant Blue staining were used again to compare the purities of the final protein preparations.

## Substrate kinetic studies with purified mPcvt2 $\alpha$ and mPcvt2 $\beta$ protein

Before the kinetic studies, multiple time courses were carried out at three different protein concentrations to ensure that CDP-ethanolamine formation was linearly related to protein amount. In addition, the molar concentration of mPcvt2 $\alpha$  was determined using spectrophotometry, and Western blotting with the anti-myc antibody followed by densitometry (data not shown) was used to equalize the molar amounts of each enzyme used in the experiments. Enzyme activity assays were carried out as described (23), with CTP at a fixed concentration of 2 mM and unlabeled phosphoethanolamine varying from 31.25  $\mu$ M to 1.0 mM. [ $^{14}$ C]phosphoethanolamine was used at a final specific activity of 0.2  $\mu$ Ci/ $\mu$ mol. All reactions were incubated at 37°C for 18 min, followed by inactivation by boiling for 2 min. Thin-layer chromatography and liquid scintillation analysis were performed as described above. Experimental data were plotted as reaction velocity (*V*) versus phosphoethanolamine concentration ([P-*etn*]) using GraphPad Prism version 4.00 for Windows (GraphPad Software), and  $K_m$  ( $\mu$ M) and  $V_{max}$  (nmol/min/ $\mu$ mol enzyme) were calculated after fitting the experimental data into a hyperbolic form of the Michaelis-Menten equation. Each experimental point on the curve represents the mean  $\pm$  SD of six replicates from two independent experiments.

Substrate kinetics were then determined with CTP as the variable substrate and [P-*etn*] fixed at 250, 500, and 1,000  $\mu$ M in turn. CTP concentration was varied from 3.125 to 1,000  $\mu$ M in each experiment. The final specific activity of [ $^{14}$ C]phosphoethanolamine used was 0.2, 0.4, or 0.8  $\mu$ Ci/ $\mu$ mol. Linear transformations of the data were carried out using GraphPad software to produce double reciprocal plots. All CTP experiments were performed twice in triplicate.

## Electrophoresis, immunoblotting and gel filtration

For the identification of expressed mPcvt2 $\alpha$  and mPcvt2 $\beta$  proteins under denaturing conditions, 10–50  $\mu$ g of total cell proteins was separated by 12% SDS-PAGE, transferred to polyvinylidene difluoride membranes, and immunoblotted with anti-His (Invitrogen) or anti-Pcvt2<sub>total</sub> (designed by us to recognize the epitope VTKAHHSSQEMSSSEYRE, common to both isoforms). For native

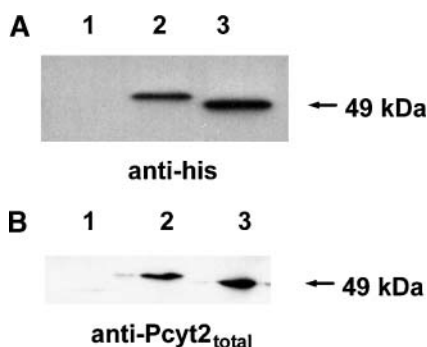


**Fig. 1.** A, B: Detection of mPcvt2 $\alpha$ -myc-His and mPcvt2 $\beta$ -myc-His expressed in COS-7 cells. Cells in 60 mm dishes were transfected with 5  $\mu$ g of empty vector or pcDNA4/myc-His containing either murine CTP:phosphoethanolamine cytidyltransferase (mPcvt2)  $\alpha$  or  $\beta$  cDNA using 20  $\mu$ l of Lipofectamine. Total cell lysates were prepared at 48 h after transfection, and proteins (10–50  $\mu$ g) were separated through 12% SDS-polyacrylamide gels, transferred to polyvinylidene difluoride membranes, and immunoblotted using antibodies as indicated. Lane 1, vector control; lane 2, mPcvt2 $\alpha$ -myc-His; lane 3, mPcvt2 $\beta$ -myc-His.

PAGE, total cell proteins (50  $\mu$ g) were separated through a 4–20% acrylamide gradient and immunoprobed as described above for denaturing gels. Samples of purified mPcvt2 $\alpha$  and mPcvt2 $\beta$  were subjected to gel filtration chromatography on a BioGel P60 (Bio-Rad) column. The void volume of the column was first determined using BSA as a standard. Elution of mPcvt2 was monitored by Western blotting with anti-myc antibody (Invitrogen).

## Immunoprecipitation

For coimmunoprecipitation studies, COS-7 cells were transfected with 4  $\mu$ g each of mPcvt2 $\alpha$ -V5-His and mPcvt2 $\beta$ -myc-His per 60 mm dish. Cells were harvested in a lysis buffer, and 500  $\mu$ g of total protein was precleared with 50  $\mu$ l of protein G agarose (Sigma) and immunoprecipitated with a 1:100 dilution of anti-V5 (Invitrogen). The final pellet was resuspended in 50  $\mu$ l of non-reducing sample buffer and boiled for 5 min. SDS-PAGE and Western blotting of total cell lysates, immunoprecipitation

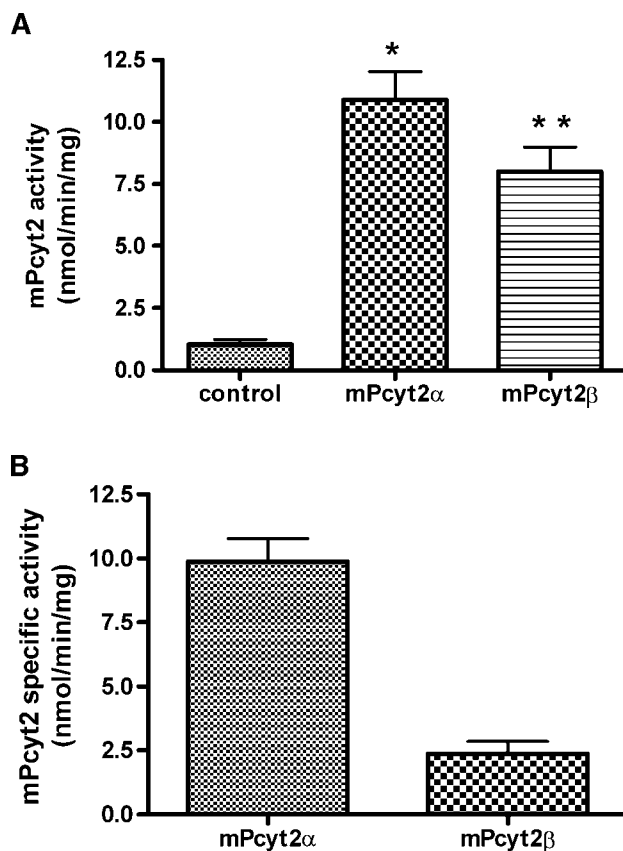


**Fig. 2.** A: In vitro activity of mPcvt2 $\alpha$  and mPcvt2 $\beta$ . COS-7 cells were transfected with 5  $\mu$ g of empty vector or with pcDNA4/myc-His containing either mPcvt2 $\alpha$  or mPcvt2 $\beta$  cDNA. Cells were harvested after 48 h, and 13,000 *g* supernatants were assayed for mPcvt2 activity as described (15), except that commercially available [ $^{14}$ C]phosphoethanolamine (American Radiolabeled Chemicals) was used at a final specific activity of 2  $\mu$ Ci/ $\mu$ mol. Results are means  $\pm$  SD of three independent experiments expressed as nmol/min/mg total protein. \* Significantly different from control ( $P < 0.001$ ); \*\* significantly different from both control and Pcv2 $\alpha$  ( $P < 0.002$ ). B: Total Pcv2 activity of the  $\alpha$  and  $\beta$  overexpressors normalized for the amount of mPcvt2 present, as determined by densitometry, and after subtraction of baseline Pcv2 activity. Results are means  $\pm$  SD. The adjusted mean activities of the  $\alpha$  and  $\beta$  isoforms were  $9.883 \pm 0.9084$  and  $2.375 \pm 0.4867$  nmol/min/mg, respectively, a significant 4-fold difference ( $P < 0.002$ ).



supernatant, and immunoprecipitation fractions were carried out using both anti-V5 and anti-myc (Invitrogen).

### Tissue-specific expression of mPcyt2 $\alpha$ and mPcyt2 $\beta$ mRNA

We initially determined the total mRNA expression and enzyme activity of mPcyt2 (22). Here, the expression patterns of mPcyt2 $\alpha$  and mPcyt2 $\beta$  mRNAs were examined in various mouse tissues. The brain, adipose, heart, kidney, liver, and skeletal muscle were dissected from three adult female C57BL/6 mice, flash-frozen in liquid nitrogen, and stored at  $-80^{\circ}\text{C}$  until RNA was extracted. Total RNA isolation and first-strand cDNA synthesis using TRIzol (Invitrogen) and SuperScript II reverse transcriptase (Invitrogen) were carried out under standard conditions. To avoid complications arising from differing reaction efficiencies, a single primer set (F6, 5'-ggagatgtcctctgagtaccg-3'; R7, 5'-ggcaccagccacatagatgac-3') was chosen for simultaneous amplification of both isoforms. The region targeted by these primers includes the alternatively spliced exon 7, producing amplified fragments of 224 and 170 bp for mPcyt2 $\alpha$  and mPcyt2 $\beta$ , respectively. PCR amplification was carried out for 36 cycles with a 30 s annealing step at  $62^{\circ}\text{C}$ . A 450 bp fragment of GAPDH was used as an internal control and amplified for 22 cycles with primer annealing at  $58^{\circ}\text{C}$ . The primers used were GAPDH-FP (5'-tccaccacctgtgctgta-3') and GAPDH-RP (5'-accacgtccatgcatcac-3'). The band densities of all

DNA fragments were determined using the Scion Image densitometry program, and all ratios are expressed as means  $\pm$  SD of three individual mice assayed in duplicate.

### Statistics

All statistical analyses were performed using GraphPad Prism version 4.00 for Windows (GraphPad Software). To evaluate the differences in enzyme activities and metabolic labeling, the paired and unpaired Student's *t*-test, respectively, were used. To test for goodness of fit of the enzyme data to the Michaelis-Menten hyperbolic function, a least sum of squares test was used. For differences in mRNA expression between tissues, one-way ANOVA followed by Dunnett's multiple pairwise comparison was used. Differences were considered significant at  $P < 0.05$ .

## RESULTS

### Overexpressed mPcyt2 $\alpha$ -myc-His and mPcyt2 $\beta$ -myc-His differ in activity

Results of the functional expression of myc-His-tagged mPcyt2 $\alpha$  and mPcyt2 $\beta$  are shown in Figs. 1, 2. Western blotting using the anti-histidine antibody showed that the mPcyt2 $\beta$  protein had an apparent molecular mass of

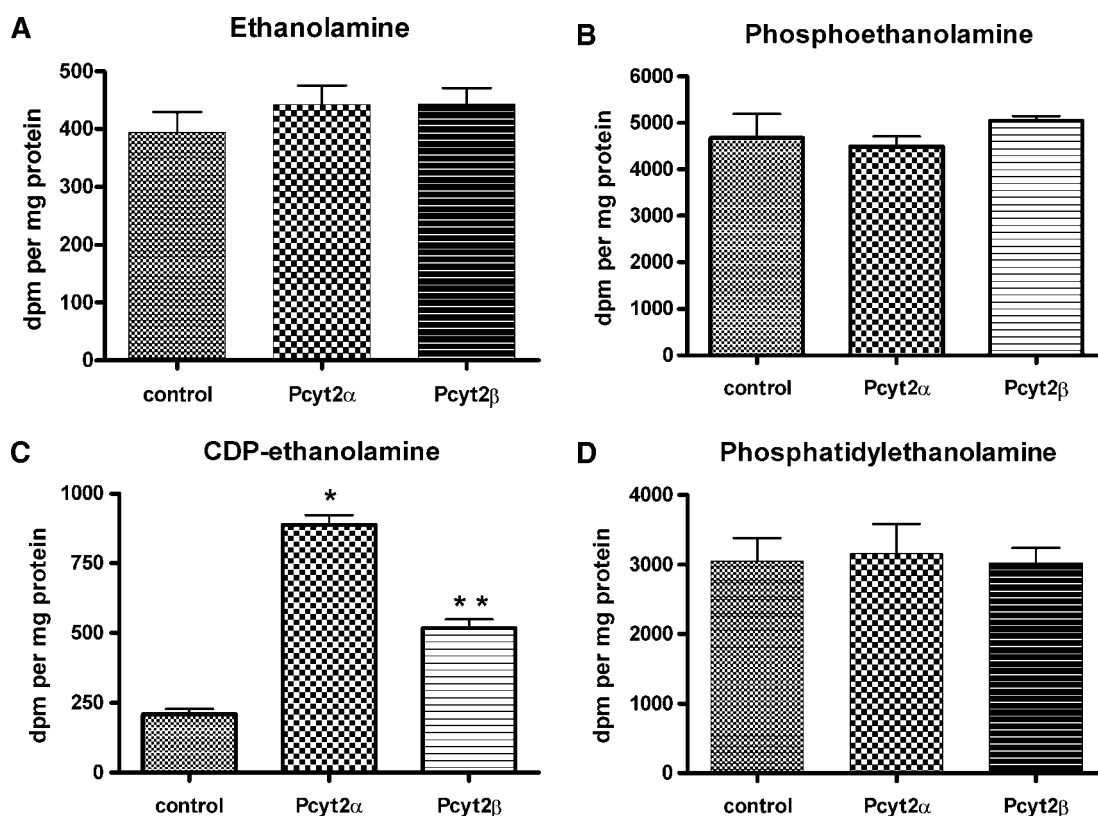


**Fig. 3.** Incorporation of [ $^{14}\text{C}$ ]ethanolamine (A) into phosphoethanolamine (B), CDP-ethanolamine (C), and phosphatidylethanolamine (PE) (D). COS-7 cells in 35 mm dishes were transfected with 2.5  $\mu\text{g}$  of empty vector or with pcDNA4/myc-His containing either mPcyt2 $\alpha$  or mPcyt2 $\beta$  cDNA using 10  $\mu\text{l}$  of Lipofectamine. Forty-six hours after transfection, cells were incubated for 2 h with 50  $\mu\text{M}$  ethanolamine and for 30 min with [ $^{14}\text{C}$ ]ethanolamine (0.2  $\mu\text{Ci}/\text{well}$ ) in the presence of 50  $\mu\text{M}$  unlabeled ethanolamine. Lipid and water-soluble fractions were separated by the method of Bligh and Dyer (24), and the methanol-water phase-soluble metabolites were resolved on Silica Gel G plates in methanol/0.5% NaCl/ammonia (50:50:5). All metabolites were visualized with 2% ninhydrin. Individual spots were subjected to liquid scintillation analysis. Total PE was determined from the chloroform phase. Results for water-soluble intermediates are means  $\pm$  SD of three experiments performed in triplicate. For PE, means are of two experiments in duplicate. \* Significantly different from control ( $P < 0.0001$ ); \*\* significantly different from both control and mPcyt2 $\alpha$  ( $P < 0.002$ ).

~49 kDa, whereas mPcyt2 $\alpha$  appeared slightly larger (Fig. 1A), indicative of the additional 18 amino acid peptide it contains (22). Western blotting with Pcyt2<sub>total</sub> antibody (Fig. 1B) was then used to confirm the identities of the expressed proteins. The total Pcyt2 activities per milligram of total cell protein in control cells (baseline) and mPcyt2 $\alpha$  and mPcyt2 $\beta$  overexpressors are depicted in Fig. 2A. Densitometry was performed on the Western blot shown in Fig. 1A, and the total Pcyt2 activity of the  $\alpha$  and  $\beta$  overexpressors was normalized for the amount of tagged mPcyt2 present, after subtraction of the baseline Pcyt2 activity in vector control cells. Figure 2B shows the specific activities of mPcyt2 $\alpha$  and mPcyt2 $\beta$  per milligram of total cell protein adjusted for mPcyt2 expression level. The adjusted mean activities of the  $\alpha$  and  $\beta$  isoforms were  $9.883 \pm 0.9084$  and  $2.375 \pm 0.4867$  nmol/min/mg, respectively, a significant 4-fold difference ( $P < 0.002$ ).

### Overexpression of mPcyt2 $\alpha$ and mPcyt2 $\beta$ increases the synthesis of CDP-ethanolamine

Results of metabolic labeling experiments, in which [ $^{14}$ C]ethanolamine was incorporated into the Kennedy pathway, are shown in Fig. 3. COS-7 cells transfected with control vector, mPcyt2 $\alpha$ -myc-His, or mPcyt2 $\beta$ -myc-His were pulse-labeled for 30 min with [ $^{14}$ C]ethanolamine, and the production of water-soluble PE precursors and PE were compared. Figure 3A, B show no significant differences in radiolabeled ethanolamine and phosphoethanolamine (the immediate precursor of CDP-ethanolamine and a substrate of mPcyt2). As expected from the data in Fig. 2, the expression of mPcyt2 $\alpha$  and mPcyt2 $\beta$  resulted in 4.2- and 2.5-fold increases in the labeling of their immediate product CDP-ethanolamine (Fig. 3C). The amount of CDP-ethanolamine formed in 30 min of labeling when mPcyt2 $\alpha$  was overexpressed was 1.7 times that of cells expressing the  $\beta$  form, agreeing closely with the in vitro activity data (Fig. 2). Lastly, overexpression of either form of mPcyt2 had no effect on the rate of PE formation (Fig. 3D). This was likely because the reaction catalyzed by ethanolamine phosphotransferase, the last enzymatic step in the Kennedy pathway, is limited by the supply of diacylglycerol (25).

### Purified mPcyt2 $\alpha$ and mPcyt2 $\beta$ differ in their kinetic properties

Figure 4 shows the relative purities of mPcyt2 $\alpha$  and mPcyt2 $\beta$  proteins. Multiple protein bands were apparent in the whole cell lysates (Fig. 4, lanes 1, 3). For each isoform, a single band was apparent (Fig. 4, lanes 2, 4) after purification and dialysis, as described in Materials and Methods. By comparing the activities per milligram of total cell protein in crude lysates with those of known quantities of pure protein, determined spectrophotometrically using a standard protein curve, we estimated a minimum 128-fold purification of the enzyme activity. Before kinetic experiments were performed, the activities of the final protein preparations were determined, and activity assays were performed at multiple time points with several different protein concentrations to establish the linearity of the

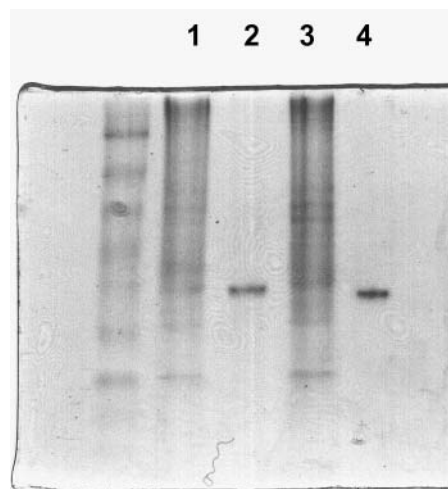


**Fig. 4.** Relative purity of mPcyt2 $\alpha$  and mPcyt2 $\beta$  preparations. Ten 10 cm culture dishes of COS-7 cells were transfected with mPcyt2 $\alpha$  or mPcyt2 $\beta$  in pcDNA4/myc-His. Cells were harvested after 48 h, and cleared lysates were applied to a Ni-NTA Superflow (Qiagen) column. The column was washed four times, and histidine-tagged proteins were eluted in multiple fractions. Pure protein fractions were dialyzed against 500 volumes of dialysis buffer, as described in Materials and Methods, and the final preparations were analyzed by SDS-PAGE and Coomassie Brilliant Blue staining. Lane 1, cleared lysate; lane 2, purified mPcyt2 $\alpha$ ; lane 3, cleared lysate; lane 4, purified mPcyt2 $\beta$ .

reaction with protein amount and time. Figure 5A shows saturation curves after plotting of the reaction velocity in nmol/min/ $\mu$ mol enzyme as a function of [P-*etn*] for both mPcyt2 $\alpha$  and mPcyt2 $\beta$ . Curve-fitting of velocity data to the Michaelis-Menten equation indicated that the two Pcyt2 isoforms were functionally distinct proteins, with differences in both substrate affinity and the rate of catalytic turnover. The  $K_m$  of mPcyt2 $\alpha$  for phosphoethanolamine was 318.4  $\mu$ M, compared with 140.3  $\mu$ M for mPcyt2 $\beta$ . The maximal velocities of the  $\alpha$  and  $\beta$  isoforms were 138 and 114.4 nmol/min/ $\mu$ mol enzyme, respectively. Figure 5B, C show the saturation curves obtained when CTP concentration was varied from 31.25 to 1,000  $\mu$ M at several fixed concentrations of phosphoethanolamine. When 1 mM phosphoethanolamine was used, the  $K_m$  of mPcyt2 $\alpha$  for CTP was 102  $\mu$ M and that of mPcyt2 $\beta$  was 84.09  $\mu$ M. Double reciprocal plots of the same data from Fig. 5B, C resulted in a series of lines intersecting at a common point (Fig. 5D, E), indicative of a sequential reaction mechanism.

### mPcyt2 $\alpha$ and mPcyt2 $\beta$ associate as homodimers and heterodimers

Using native gradient PAGE and the Pcyt2<sub>total</sub> antibody, we investigated the formation of higher order protein complexes by mPcyt2 $\alpha$  and mPcyt2 $\beta$  expressed individually and together in COS-7 cells. As shown in Fig. 6A (lane 2), myc-His-tagged mPcyt2 $\alpha$  appears as a single band of ~108 kDa, which represents the  $\alpha/\alpha$  homodimer. Under the same conditions, mPcyt2 $\beta$  (Fig. 6A, lane 3) appears as two bands, the weaker of the two at ~110 kDa and the stronger one

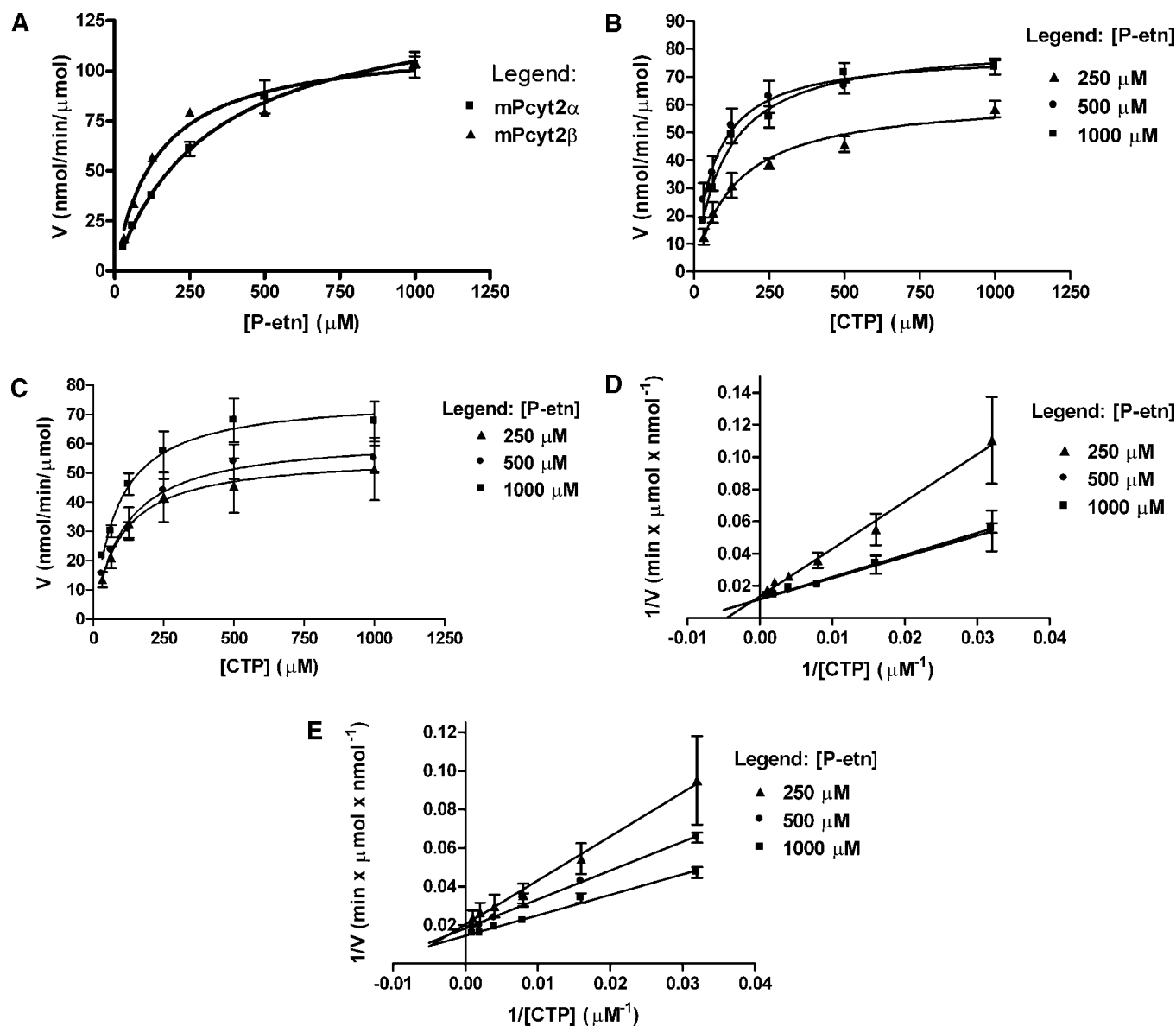


**Fig. 5.** A: Substrate kinetics of mPcyt2 $\alpha$  and mPcyt2 $\beta$  with CTP at a fixed concentration of 2 mM and phosphoethanolamine concentration ([P-ethn]) varying from 31.25  $\mu$ M to 1.0 mM. [ $^{14}$ C]phosphoethanolamine was used at a final specific activity of 0.2  $\mu$ Ci/ $\mu$ mol. B, C: CTP kinetics of mPcyt2 $\alpha$  (B) and mPcyt2 $\beta$  (C) with phosphoethanolamine at fixed concentrations of 250, 500, and 1,000  $\mu$ M and CTP varying from 31.25  $\mu$ M to 1.0 mM. [ $^{14}$ C]phosphoethanolamine was used at a final specific activity of 0.2–0.8  $\mu$ Ci/ $\mu$ mol. D, E: Double reciprocal plots of the data in B, C. All reactions were incubated at 37°C for 18 min. Curve-fitting to the hyperbolic Michaelis-Menten equation and Lineweaver-Burk transformations of experimental data were done using GraphPad Prism software. All experiments were performed twice in triplicate. Results are means  $\pm$  SD.

at  $\sim$ 90 kDa. Based on the estimated monomeric size of  $\sim$ 50 kDa (Fig. 1), these results show that both isoforms associate as homodimers and that mPcyt2 $\beta$  has at least two  $\beta/\beta$  mobility variants, the cause of which is yet unknown. When both isoforms were expressed together (Fig. 6A, lane 4), complexes that electrophoretically reassembled  $\beta/\beta$  homodimers were apparent, although the presence of  $\alpha/\alpha$  homodimers and  $\alpha/\beta$  heterodimers could not be ruled out.

Gel filtration chromatography was performed on purified mPcyt2 $\alpha$  and mPcyt2 $\beta$  to confirm the dimeric structure of both isoforms. When each protein was sub-

jected to gel filtration on a column with an exclusion limit of 60 kDa, all of the eluted protein was present in fractions corresponding to the void volume of the column (1.8 ml), as was determined previously using BSA. All 150  $\mu$ l fractions obtained by gel filtration of mPcyt2 $\alpha$  and mPcyt2 $\beta$  were analyzed for the presence of tagged protein using the anti-myc antibody, and those that contained the protein are shown (Fig. 6B, C). No protein was detected in any of the subsequent fractions (data not shown). These results indicate that both mPcyt2 isoforms were excluded from the gel and therefore must

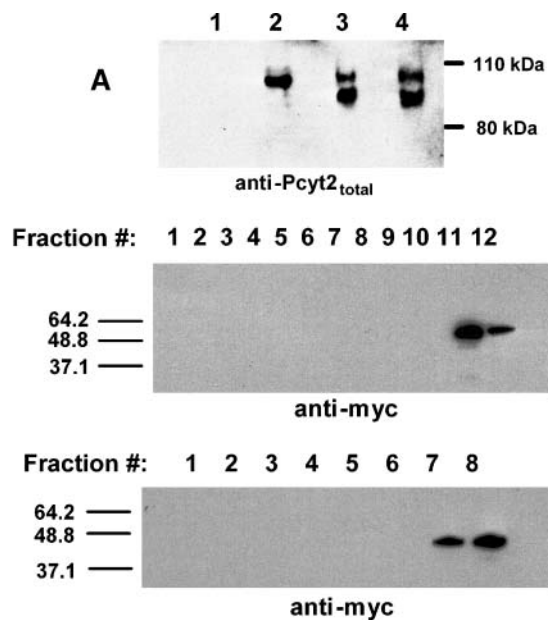


**Fig. 6.** A: Nondenaturing gradient PAGE of mPcvt2 dimers. mPcvt2 $\alpha$  and mPcvt2 $\beta$  were expressed separately and together in COS-7 cells. Whole cell lysates were subjected to nondenaturing PAGE in a 4–20% gradient, transferred to polyvinylidene difluoride membranes, and immunoblotted with antibody to total Pcvt2. Lane 1, vector control cells; lane 2, cells overexpressing mPcvt2 $\alpha$ -myc-His; lane 3, cells overexpressing mPcvt2 $\beta$ -myc-His; lane 4, cells overexpressing both mPcvt2 $\alpha$ -V5-His and mPcvt2 $\beta$ -myc-His. B, C: Western blot with anti-myc antibody after gel filtration chromatography of mPcvt2 $\alpha$  (B) and mPcvt2 $\beta$  (C) dimers. Myc-His-tagged and purified mPcvt2 $\alpha$  and mPcvt2 $\beta$  were subjected to gel filtration chromatography in a Bio-Gel P60 column, and the fractions were analyzed by Western blotting with anti-myc antibody.

have a molecular mass of >60 kDa. This would only be possible if the proteins were in dimeric form, as the molecular mass of the  $\alpha$  and  $\beta$  monomers would be  $\sim$ 51 and  $\sim$ 49 kDa.

To further determine whether mPcvt2 $\alpha$ / $\beta$  heterodimers could form, we coexpressed mPcvt2 $\alpha$ -V5-His and mPcvt2 $\beta$ -myc-His, then performed immunoprecipitation with anti-V5 and detection with anti-myc. As shown in **Fig. 7A**, the myc epitope was clearly detected in the anti-V5 precipitates, indicating an mPcvt2 $\alpha$ / $\beta$  association. Myc was also detected in the total lysates of cotransfected cells and the immunoprecipitation supernatants but was absent from control cells. Western blotting with anti-V5 (**Fig. 7B**) revealed that mPcvt2 $\alpha$ -V5 was present in the total lysates and precipitates but absent from the supernatant, indicating that the V5 antibody was completely effective in pulling down all of the expressed mPcvt2 $\alpha$ -V5 protein. An additional Western blot of the lysates from cells overexpressing mPcvt2 $\alpha$ -V5, mPcvt2 $\beta$ -myc-His, or both constructs together was performed to show the specificity of the anti-V5 antibody for proteins with a V5 tag. Because no mPcvt2 $\beta$ -myc-His was detected with this antibody, a nonspecific immunoprecipitation of mPcvt2 $\beta$ -myc-His was not likely.

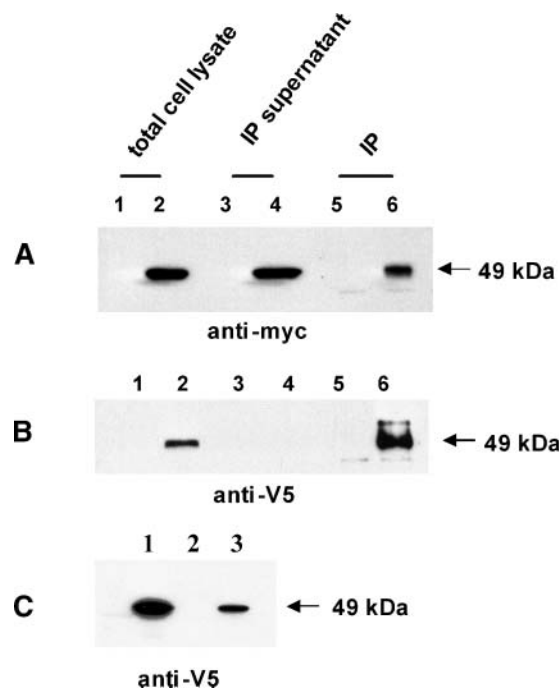


**Fig. 7.** Immunoprecipitation of mPcvt2 $\alpha$ / $\beta$  complexes. A, B: Lysates from cells cotransfected with mPcvt2 $\alpha$ -V5-His and mPcvt2 $\beta$ -myc-His were subjected to immunoprecipitation (IP) using anti-V5, and Western blotting was carried out using anti-myc (A) and anti-V5 (B). Lanes 1, 3, 5, vector control cells; lanes 2, 4, 6, cotransfected cells. C: Western blot showing the specificity of anti-V5 for the V5-tagged protein. Lane 1, lysates from cells overexpressing mPcvt2 $\alpha$ -V5-His; lane 2, lysates from mPcvt2 $\beta$ -myc-His overexpressors; lane 3, lysates from cells overexpressing both myc and V5 constructs.

#### Alternative splicing of mPcvt2 is tissue-specific

Several mouse tissues were analyzed for the expression of mPcvt2 $\alpha$  and mPcvt2 $\beta$  mRNAs (**Fig. 8**). Because the single primer pair we used should anneal equally well to the priming sites (on either side of the alternatively spliced exon 7) in both mPcvt2 mRNAs, it is reasonable to compare the mRNA abundance of two splice variants within a tissue using this type of assay, as was done for the SMRT gene by Malartre, Short, and Sharpe (26). Of all tissues examined, liver and adipose showed the highest level of mPcvt2 $\alpha$ , whereas the lowest expression was found in muscle, brain, and heart (**Fig. 8A**). The level of mPcvt2 $\beta$  mRNA was relatively low in all tissues (**Fig. 8B**), in keeping with the previous observation that mPcvt2 $\alpha$  was the more prominent of the two isoforms in the murine expressed sequence database (22). Considered together with the relatively large variation observed in mPcvt2 $\alpha$  mRNA expression (**Fig. 8A**) and the higher catalytic activity of  $\alpha$  relative to  $\beta$  (**Figs. 2, 3**), these observations suggest that in the mouse, variations in total Pcvt2 activity are largely determined by the expression of the  $\alpha$  form. In a few tissues, namely brain, heart, and muscle, appreciable amounts of mPcvt2 $\beta$  could additionally modulate mPcvt2 function. When the ratios of  $\alpha$ / $\beta$  mRNA abundance were calculated, the liver, kidney, and fat emerged with the highest amounts (3.2, 3.1, and 2.6),



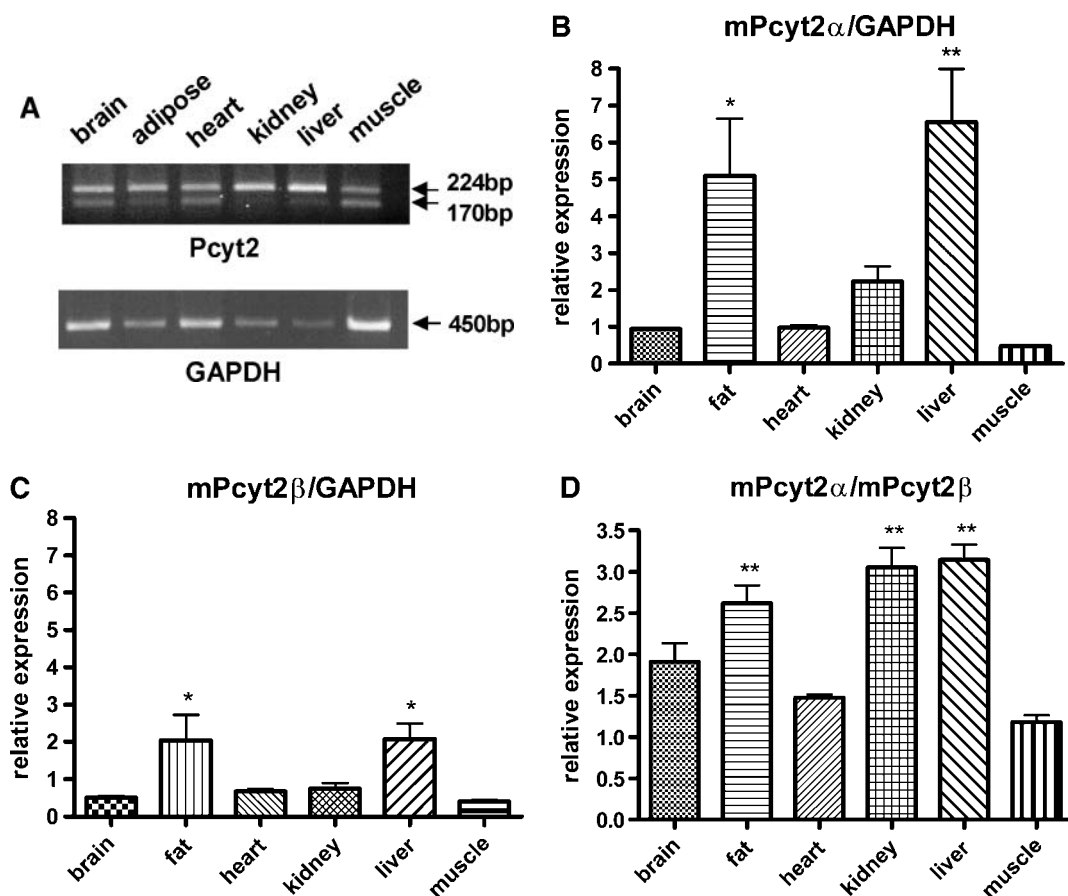


**Fig. 8.** A: Tissue-specific distribution of mPcyt2 $\alpha$  and mPcyt2 $\beta$  transcripts. PCR primers flanking the alternatively spliced exon 7 were used to amplify 224 and 170 bp fragments of the mPcyt2 $\alpha$  and mPcyt2 $\beta$  cDNAs, respectively. In B and C, mPcyt2 mRNA expression was normalized to that of GAPDH. D: Ratio of mPcyt2 $\alpha$  to mPcyt2 $\beta$  expression. Results are means  $\pm$  SD of three individual animals, each analyzed in duplicate. ANOVA was performed at  $P < 0.05$  (\*) or at  $P < 0.01$  (\*\*) relative to muscle.

whereas muscle had nearly equal amounts of each variant (Fig. 8).

## DISCUSSION

We report for the first time the functional expression, purification, and kinetics of two structurally distinct isoforms of mPcyt2. The aims of our study were to characterize the function and differences between these two proteins and to gain insight into the role of alternative splicing in the regulation of enzyme function. Results obtained using three independent approaches (in vitro activity assays, metabolic labeling, and kinetic assays of purified proteins) demonstrate that the catalytic activities of Pcyt2 $\alpha$  and Pcyt2 $\beta$  isoforms differ significantly. Because the only structural difference between the mPcyt2 $\alpha$  and mPcyt2 $\beta$  proteins used in these studies is the 18 amino acid "linker peptide" (180-PPHPTPAGDTLSSEVSSQ-197) that is present only in the  $\alpha$  variant, it is highly probable that this peptide is a major factor in the modulation of mPcyt2 function. This study provides the first direct evidence linking this particular exon-skipping mechanism to the functional consequence of decreased enzymatic

activity. Several observations led to this hypothesis. First, the linker peptide is situated between two conserved catalytic domains (17), indicating that its presence or absence would affect the molecular distance between the two putative catalytic sites. Second, our examination of the amino acid composition of the linker peptide indicated a loop sequence containing four proline residues, which are known to introduce random coil structures between  $\alpha$ -helical and/or  $\beta$ -sheet domains (27). Third, a similar alternative splicing mechanism for the Pcyt2 gene is highly conserved throughout the animal kingdom, suggesting that the presence of Pcyt2 $\alpha$  and Pcyt2 $\beta$  isoforms bears evolutionary significance (22). Our kinetic analyses indicate that mPcyt2 $\alpha$  has both a lower affinity for phosphoethanolamine (indicated by the  $K_m$  values) and a higher maximal velocity than mPcyt2 $\beta$  when phosphoethanolamine and CTP are at saturating conditions.


When rat Pcyt2 was initially purified by Sundler (5), the behavior of the protein on gel chromatography indicated a dimeric structure. Using a combination of native gradient PAGE, gel filtration chromatography, and Western blotting, we evaluated the individual ability of Pcyt2 $\alpha$  and Pcyt2 $\beta$  to form homodimers. Because all bands that were detected using the Pcyt2 antibody were well above the



estimated monomeric sizes of 49 and 51 kDa, we conclude that monomeric Pcyt2 does not exist or is not present in appreciable quantities and that each isoform is able to associate into homodimers in the absence of the other. In addition, gel filtration chromatography indicated that both isoforms existed only as dimers. Our immunoprecipitation experiments on coexpressed proteins, in which myc-tagged mPcyt2 $\beta$  was shown to coprecipitate with V5-tagged mPcyt2 $\alpha$ , provide the first known evidence of a heteromeric Pcyt2 $\alpha$ / $\beta$  association.

The possibility exists that homodimerization and heterodimerization itself play a role in the overall regulation of Pcyt2 activity. There are two levels at which this could occur. The first is the activity of the spliceosome complex toward the mPcyt2 primary mRNA transcript, which would directly influence the relative amounts of each isoform expressed. This would in turn determine, in whole or in part, the position of the dimerization equilibrium (the proportion of Pcyt2 dimers as  $\alpha/\alpha$ ,  $\alpha/\beta$ , and  $\beta/\beta$ ). Results from our multiple tissue mRNA expression study indicated that the relative levels of mPcyt2 $\alpha$  and Pcyt2 $\beta$  transcripts do indeed vary from one tissue to another, as is often the case with alternatively spliced mRNAs (28).

The second possibility is that there is posttranslational control over the formation of dimers. This process could be modulated by structural aspects of the linker peptide, such as its phosphorylation state (L. Zhu and M. Bakovic, unpublished data), that could either promote or inhibit dimer formation between like or unlike monomers. In the theoretical case in which equal amounts of  $\alpha$  and  $\beta$  monomer units were expressed, one would expect  $\alpha/\alpha$ ,  $\alpha/\beta$ , and  $\beta/\beta$  dimers to occur in ratios of 1:2:1 if the process of dimerization was completely random. If, however, the affinity of the  $\alpha/\alpha$  or  $\beta/\beta$  association far exceeded that of the  $\alpha/\beta$  association, then a greater than expected proportion of the total enzyme molecules would be in homodimeric form and the net activity should be close to the average of activities we observed for homodimers. If, on the other hand, the tendency toward heterodimerization was greater than or equal to the affinity of like monomer units for each other, then the net activity would depend on both the (as yet unknown) catalytic properties of the heterodimer and the extent of heterodimerization.

The existence of multiple isoforms among enzymes of the CDP-choline and CDP-ethanolamine pathways is not unique to Pcyt2. In fact, there is a known functional redundancy at each enzymatic step, with at least two isoforms encoded by at least two different genes for choline/ethanolamine kinase (29), ethanolamine kinase (30, 31), CTP:phosphocholine cytidyltransferase (32), and choline/ethanolamine phosphotransferase (33). In this regard, Pcyt2 is no different, except that both isoforms are encoded by the same gene and, to the best of current knowledge, only alternative splicing is responsible for enzyme diversity in Pcyt2. We have just begun to characterize two isoforms of Pcyt2, about which little has been revealed to date. This enzyme can now be included in a growing list of proteins for which alternative splicing generates functional diversity. 

The authors thank the Canadian Institutes for Health Research (Grant 129345 to M.B.) and the Ontario Graduate Scholarship program (for financial support to A.T.).

## REFERENCES

- Kennedy, E. P., and S. B. Weiss. 1956. The function of cytidine coenzymes in the biosynthesis of phospholipids. *J. Biol. Chem.* **222**: 193–214.
- Bladergroen, B. A., and L. M. G. van Golde. 1997. CTP:phosphoethanolamine cytidyltransferase. *Biochim. Biophys. Acta.* **1348**: 91–99.
- Tijburg, L. B. M., M. J. H. Geelen, and L. M. G. van Golde. 1989. Regulation of the biosynthesis of triacylglycerol, phosphatidylcholine and phosphatidylethanolamine in the liver. *Biochim. Biophys. Acta.* **1004**: 1–19.
- Wilson, J. D., K. D. Gibson, and S. Udenfriend. 1960. Studies on the conversion in vitro of serine to ethanolamine by rat liver and brain. *J. Biol. Chem.* **235**: 3539–3543.
- Sundler, R. 1975. Ethanolaminephosphate cytidyltransferase: purification and characterization of the enzyme from rat liver. *J. Biol. Chem.* **250**: 8585–8590.
- Ellens, H., D. P. Siegel, D. Alford, P. L. Yeagle, L. Boni, L. J. Lis, P. J. Quinn, and J. Bentz. 1989. Membrane fusion and inverted phases. *Biochemistry.* **28**: 3692–3703.
- Emoto, K., T. Kobayashi, A. Yamaji, H. Aizawa, I. Yahara, K. Inoue, and M. Umeda. 1996. Redistribution of phosphatidylethanolamine at the cleavage furrow of dividing cells during cytokinesis. *Proc. Natl. Acad. Sci. USA.* **93**: 12867–12872.
- Farge, E., D. M. Ojcius, A. Subtil, and A. Dautry-Varsat. 1999. Enhancement of endocytosis due to aminophospholipid transport across the plasma membrane of living cells. *Am. J. Physiol.* **276**: C725–C733.
- Knowles, D. W., L. Tilley, N. Mohandas, and J. A. Chasis. 1997. Erythrocyte membrane vesiculation: model for the molecular mechanism of protein sorting. *Proc. Natl. Acad. Sci. USA.* **94**: 12969–12974.
- Ichimura, Y., T. Kirisako, T. Takao, Y. Satomi, Y. Shimonishi, N. Ishihara, N. Mizushima, I. Tanida, E. Kominami, M. Ohsumi, et al. 2000. A ubiquitin-like system mediates protein lipidation. *Nature.* **408**: 488–492.
- Asai, K., T. Hirabayashi, T. Houjou, N. Uozumi, R. Taguchi, and T. Shimizu. 2003. Human group IVC phospholipase A2 (cPLA2g). *J. Biol. Chem.* **278**: 8809–8814.
- Arthur, G., and L. Page. 1991. Synthesis of phosphatidylethanolamine and ethanolamine plasmalogen by the CDP-ethanolamine and decarboxylase pathways in rat heart, kidney and liver. *Biochem. J.* **273**: 121–125.
- Brites, P., H. R. Waterham, and R. J. A. Wanders. 2004. Functions and biosynthesis of plasmalogens in health and disease. *Biochim. Biophys. Acta.* **1636**: 219–231.
- Schrakamp, G., R. B. H. Schutgens, R. J. A. Wanders, H. S. A. Heymans, J. M. Tager, and H. Van den Bosch. 1985. The cerebro-hepato-renal (Zellweger) syndrome. Impaired de novo biosynthesis of plasmalogens in cultured skin fibroblasts. *Biochim. Biophys. Acta.* **833**: 170–174.
- Vance, J. E., and D. E. Vance. 2005. Metabolic insights into phospholipid function using gene-targeted mice. *J. Biol. Chem.* **280**: 10877–10880.
- Jackowski, S., and P. Fagone. 2005. CTP:phosphocholine cytidyltransferase: paving the way from gene to membrane. *J. Biol. Chem.* **280**: 853–856.
- Min-Seok, R., Y. Kawamata, H. Nakamura, A. Ohta, and M. Takagi. 1996. Isolation and characterization of ECT1 gene encoding CTP:phosphoethanolamine cytidyltransferase of *Saccharomyces cerevisiae*. *J. Biochem. (Tokyo).* **120**: 1040–1047.
- Vermeulen, P. S., L. B. M. Tijburg, M. J. H. Geelen, and L. M. G. van Golde. 1993. Immunological characterization, lipid dependence, and subcellular localization of CTP:phosphoethanolamine cytidyltransferase purified from rat liver. *J. Biol. Chem.* **268**: 7458–7464.
- Vermeulen, P. S., M. J. H. Geelen, and L. M. G. van Golde. 1994. Substrate specificity of CTP:phosphoethanolamine cytidyltransferase purified from rat liver. *Biochim. Biophys. Acta.* **1211**: 343–349.
- Nakashima, A., K. Hosaka, and J. Nikawa. 1997. Cloning of a hu-

- man cDNA for CTP-phosphoethanolamine cytidyltransferase by complementation in vivo of a yeast mutant. *J. Biol. Chem.* **272**: 9567–9572.
21. Bladergroen, B. A., M. Houweling, M. J. H. Geelen, and L. M. G. van Golde. 1999. Cloning and expression of CTP:phosphoethanolamine cytidyltransferase cDNA from rat liver. *Biochem. J.* **343**: 107–114.
  22. Poloumienko, A., A. Cote, A. Tie Ten Quee, L. Zhu, and M. Bakovic. 2004. Genomic organization and differential splicing of the mouse and human Pcyt2 genes. *Gene.* **325**: 145–155.
  23. Tijburg, L. B. M., P. S. Vermeulen, and L. M. G. van Golde. 1992. Ethanolamine-phosphate cytidyltransferase. *Methods Enzymol.* **209**: 258–263.
  24. Bligh, E. G., and W. J. Dyer. 1959. A rapid method of total lipid extraction and purification. *Can. J. Biochem. Physiol.* **37**: 911–917.
  25. Bleijerveld, O. B., W. Klein, A. B. Vaandrager, J. B. Helms, and M. Houweling. 2004. Control of the CDP-ethanolamine pathway in mammalian cells: effect of CTP:phosphoethanolamine cytidyltransferase overexpression and the amount of intracellular diacylglycerol. *Biochem. J.* **379**: 711–719.
  26. Malartre, M., S. Short, and C. Sharpe. 2004. Alternative splicing generates multiple SMRT transcripts encoding conserved repressor domains linked to variable transcription factor interaction domains. *Nucleic Acids Res.* **32**: 4676–4686.
  27. Yang, S. T., J. Y. Lee, H. J. Kim, Y. J. Eu, S. Y. Shin, K. S. Hahm, and J. I. Kim. 2006. Contribution of a central proline in model amphipathic alpha-helical peptides to self-association, interaction with phospholipids, and antimicrobial mode of action. *FEBS J.* **273**: 4040–4054.
  28. Short, S., M. Malartre, and C. Sharpe. 2005. SMRT has tissue-specific isoform profiles that include a form containing one CoRNR box. *Biochem. Biophys. Res. Commun.* **334**: 845–852.
  29. Ishidate, K. 1997. Choline/ethanolamine kinase from mammalian tissues. *Biochim. Biophys. Acta.* **1348**: 70–78.
  30. Lykidis, A., J. Wang, M. A. Karim, and S. Jackowski. 2001. Overexpression of a mammalian ethanolamine-specific kinase accelerates the CDP-ethanolamine pathway. *J. Biol. Chem.* **276**: 2174–2179.
  31. Tian, Y., P. Jackson, C. Gunter, J. Wang, C. O. Rock, and S. Jackowski. 2006. Placental thrombosis and spontaneous fetal death in mice deficient in ethanolamine kinase 2. *J. Biol. Chem.* **281**: 28438–28449.
  32. Lykidis, A., K. G. Murti, and S. Jackowski. 1998. Cloning and characterization of a second human CTP:phosphocholine cytidyltransferase. *J. Biol. Chem.* **273**: 14022–14029.
  33. Hjeltnstad, R. H., and R. M. Bell. 1988. The sn-1,2-diacylglycerol ethanolaminephosphotransferase activity of *Saccharomyces cerevisiae*. Isolation of mutants and cloning of the EPT1 gene. *J. Biol. Chem.* **263**: 19748–19757.